ACS PHYSICAL CHEMISTRY Au
AN OPEN ACCESS JOURNAL OF THE AMERICAN CHEMICAL SOCIETY

pubs.acs.org/physchemau
Article

Coffee Silver Skin: A Useful Adsorbent Substrate for Norfloxacin Removal and Photodegradation

Domenico Cignolo, Vito Rizzi, Maria Teresa Bozzelli, Paola Fini, Andrea Petrella, Pinalysa Cosma, and Jennifer Gubitosa*

Cite This: ACS Phys. Chem Au 2025, 5, 375−386
Read Online
ACCESS | Metrics & More | Article Recommendations

ABSTRACT: This work proposes the use of Coffee Silver Skin, a by-product of coffee production, as an adsorbent substrate for the removal of the antibiotic Norfloxacin from water and assesses the possibility of regenerating it through advanced oxidation processes. In detail, the study was developed by showing the best conditions for the pollutant removal, in which the adsorption process occurred with the main involvement of electrostatic interactions. A preliminary desorption approach in the presence of salt-based solutions, i.e., NaCl and 0.1 M $MgCl_2$, was followed with the aim of desorbing the non-photodegraded Norfloxacin from the regenerated adsorbent. Therefore, indirectly, the quantitative evaluation of photodestroyed Norfloxacin was assessed according to selected working conditions: UV light, UV light/H_2O_2, UV light/TiO_2, and UV light/TiO_2/H_2O_2. Moreover, a comparison with the literature devoted to Norfloxacin photodegradation directly in water was accomplished. The use of UV light/TiO_2 occurred as the best approach for the purpose of obtaining the complete degradation of Norfloxacin in 6 h. On the other hand, the use of H_2O_2 did not improve the process. Thus, to reduce the irradiation time, Norfloxacin degradation was evaluated simultaneously during its release from the adsorbent, in a 0.1 M $MgCl_2$ solution, retrieving a similar and well-known behavior observed when the pollutant was degraded in water. In 3 h, the desorbed Norfloxacin was destroyed, enabling the recycling of Coffee Silver Skin for up to 3 cycles.

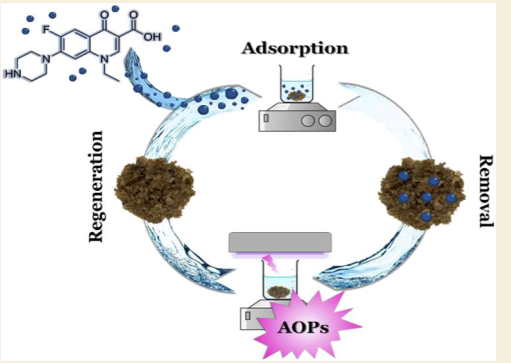

KEYWORDS: *Coffee Silver Skin, adsorption, photodegradation, Norfloxacin, advanced oxidation processes, recycling, waste and by-product management*

Antibiotics are the most frequently prescribed drugs worldwide, with a continuous increase in their usage, which has worsened the problem related to antibiotic resistance. Their large consumption is not limited to medicine; rather, they are employed also in dentistry, veterinary, and agriculture.[1] Among antibiotics, the large use of fluoroquinolones (FQs) is highlighted due to their broad-spectrum action against various pathogenic bacteria. Indeed, in the last years, their usage has increased for handling pneumonia in patients affected by SARS-CoV-2.[2] In this regard, Norfloxacin (NOR) is worth mentioning.[3] It is usually employed to treat urinary infections and prostate-related problems, both in hospital and veterinary fields, with an annual consumption of several tons, leading to being considered among the five most used antibiotics around the world.[4] Due to these large uses, NOR is commonly retrieved in water, being discharged from the effluents of hospitals, veterinary clinics, and domestic sources, and it has been detected in concentrations of μg/L or mg/L in sewage, groundwater, and surface water. However, this large presence can be toxic for humans, causing seizures, angioedema, peripheral neuropathy, tendon rupture, hallucinations, vomiting, nausea, diarrhea, hypersensitivity reactions, photosensitivity, Stevens−Johnson syndrome, and effects on the central nervous system. Moreover, it can lead to toxic effects on aquatic ecosystems, damaging them to a huge extent.[4] On these bases, NOR has been classified as a Contaminant of Emerging Concern (CEC), and it raises the need to remove this pollutant from water.[5] For this purpose, many techniques have already been explored, i.e., filtration, reverse osmosis, adsorption, coagulation−flocculation, ion exchange, advanced oxidation processes (AOPs), and biological wastewater treatments.[6−10] However, the use of some of these approaches is not strongly encouraged, exhibiting disadvantages, such as the cost of installation, chemical reagents, energy requirement, production of a high volume

Received: February 17, 2025
Revised: April 17, 2025
Accepted: April 18, 2025
Published: May 21, 2025

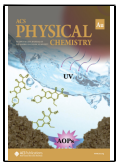

of sludge, or low efficiency and long required times.[11] On the other hand, the use of adsorption and degradation processes (especially devoted to photodegradation involving UV light, assisted by photocatalyst or oxidant agent, Fenton-like processes, persulfate-based advanced oxidation processes, and ionizing or γ-ray irradiation) could be considered the most prominent techniques for NOR removal.[4,11−22]

Specifically, adsorption can be considered an eco-friendly and cost-effective technique, more efficient than conventional methods, without requiring chemicals, high pressure or temperature, or hard operation conditions. Nonetheless, it suffers from some disadvantages: (i) it is specific for a particular pollutant or class of compounds and[23] (ii) the disposal of the used material after the adsorption could represent a serious problem. Indeed, the latter is considered a harmful secondary by-product, if not properly regenerated. To overcome these problems, the use of advanced oxidation processes (AOPs) has been largely discussed. Indeed, AOPs are considered, although the quite high associated costs, interesting nonselective methods for wastewater treatment, exhibiting high efficiency and capacity to oxidize and mineralize many organic compounds.[23,24] At the same time, the degradation of the adsorbed pollutant is an interesting option to regenerate the adsorbent, unlike the desorption of the adsorbed contaminant, which often cannot be achieved. Accordingly, the literature survey obtained from the Scopus database shows that the number of studies proposing the adsorption and/or degradation methods to remove NOR from water has increased in the past decade (Figure 1). Particularly, it seems that the use of degradation was preferred over adsorption.

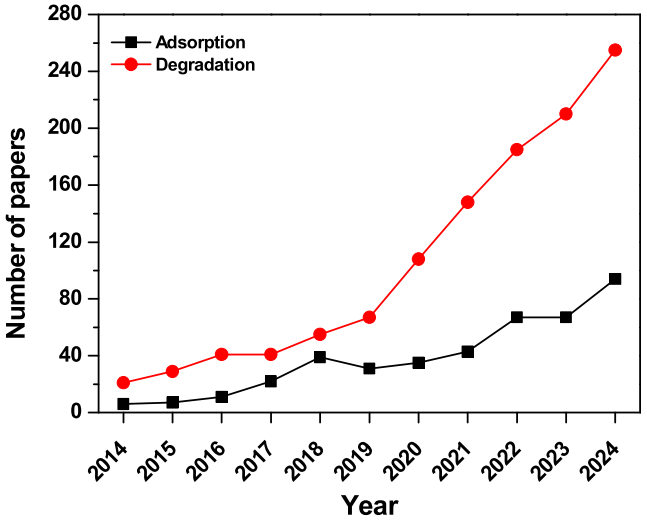

Figure 1. Number of scientific publications by year in the last 10 years about the adsorption (black line) and degradation (red line) of Norfloxacin in water. Scopus database was used.

Focusing on NOR's degradability by means of AOPs, among the available studies, the use of UV/TiO_2, UV/H_2O_2, Fenton, and Photo-Fenton is worth mentioning.[18,19,21,25] However, the main attention was devoted to the NOR degradation directly in water, with the drawback of further polluting it with secondary by-products, which could be potentially more toxic than the parent compound.

Differently, this work aimed to adsorb and then photodegrade NOR at the solid state for successfully regenerating the adsorbent, extending its lifetime. At the same time, the proposed approach enabled the possibility of destroying NOR under controlled conditions, avoiding the unwanted release of other substances into water. Specifically, Coffee Silver Skin (CSS) was adopted as an adsorbent substrate. The CSS is the thin skin covering the green coffee bean, representing the by-product obtained from roasting green coffee berries. It is collected in large amounts from the roasting factories.[26−28] However, although the Circular Economy principles encourage the use of by-products for their valorization, simultaneously lowering the environmental impact,[29,30] the reuse of CSS for different applications has not been fully explored. It has been mainly used as biomass or for the extraction of bioactive molecules, with the perspective of developing systems to obtain feed, fertilizer, microbial fermentation materials for biorefinery, and the recovery of energy by combustion.[26,31,32] On the other hand, considering its potential application for water remediation, many studies have been devoted to the general use of coffee waste, also in the form of active carbon, to remove different pollutants,[33−35] while the use of CSS has not been widely contemplated. Interestingly, Malara et al. proposed CSS as an adsorbent material to remove heavy metals.[36] Based on this background, this work contributes to suggesting a way for further valorizing CSS, using this biomass for water remediation to remove CECs, and recycling it through AOPs. Moreover, unlike similar works in the field, hard experimental conditions for pretreating CSS before its use as an adsorbent were avoided, proposing only the use of hot water, further lowering the environmental impact.[37,38] Furthermore, it is important to highlight that, regarding the use of coffee wastes in NOR removal, only biochar derived from spent coffee grounds[35] and coffee husk[38] have been reported for NOR adsorption, highlighting the importance of the present work. To get insight into the NOR's degradation, both in solid state on CSS or when released from the adsorbent and destroyed, a comparison with the well-known[19,21,39] NOR degradation in water solution was performed, unveiling the retrieved results. New horizons are thus opened with this work, showing in the literature a valid way to regenerate CSS, extending its use, according to sustainability principles.

1. EXPERIMENTAL SECTION

1.1. Materials

Coffee Silver Skin (CSS) was received by "Fattoria Gallorosso", Contrada Murge S. Andrea Snc 75024 Montescaglioso (MT). Norfloxacin, NaCl, $MgCl_2$, and H_2O_2 30% (w/w) were purchased from Sigma-Aldrich (Milan, Italy). A stock solution of 30 mg of Norfloxacin was prepared in deionized water. Aeroxide TiO_2 P25 was purchased from Evonik Industries AG.

1.2. Preparation of Adsorbent Substrate

Ten grams of a sample of Coffee Silver Skin, CSS (raw biomass), was placed in 400 mL of deionized water at 80 °C and stirred for 20 min. The washing procedure was repeated several times. Then, the biomass was dried in an oven at 60 °C until constant weight.

1.3. ATR-FTIR Spectroscopy Analyses

A Fourier transform infrared spectrometer, Shimadzu IRXross, Shimadzu Corp., was adopted to collect the ATR-FTIR spectra of CSS before and after photodegradation processes in the range of 500−4000 cm^{-1}. In particular, the dried samples were placed on the ATR crystal and pressed down using the swivel press to ensure optimal contact between the sample and the crystal. A constant

https://doi.org/10.1021/acsphyschemau.5c00013
ACS Phys. Chem Au 2025, 5, 375−386

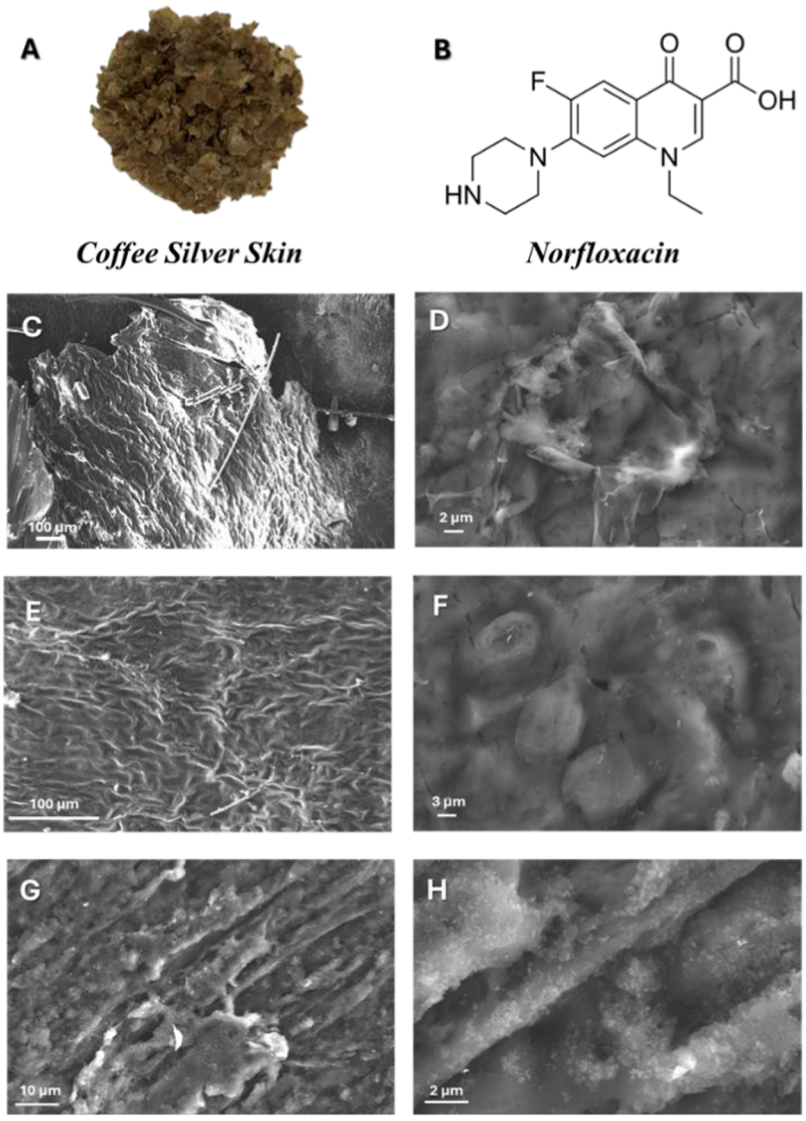

Figure 2. Camera picture of water-washed CSS (A), Norfloxacin molecular structure (B), and SEM images of raw CSS (C, D), water-washed CSS at different magnification ratios (E, F), and recycled CSS at different magnification ratios (G, H).

strength was used for each analysis. A resolution of 4 cm^{-1} was set, and 45 scans were summed for each acquisition.

1.4. Thermogravimetric Analyses (TGAs)

The thermal investigation of the adsorbent was performed using a thermogravimetric instrument (PerkinElmer Pyris 1), and analyses were performed under an inert atmosphere using nitrogen as a purge gas with a constant flow rate of 20 mL/min. Each sample was heated from 30 to 650 °C at a heating rate of 10 °C/min.

1.5. UV−vis Analyses

A Shimadzu UV-2600i UV−vis-NIR spectrophotometer was employed for monitoring the adsorption, desorption, and photodegradation processes. The UV−vis spectra of NOR solutions were acquired at different time intervals in the wavelength range 200−450 nm, at a 1 nm/s scan rate.

1.6. Scanning Electron Microscopy (SEM) Analyses

The morphology of the adsorbent samples was investigated using a Zeiss scanning electron microscope model EVO50XVP (Carl Zeiss Microscopy GmbH, Jena, Germany). The samples were fixed on aluminum stubs with colloidal graphite and then sputtered with a 30 nm thick carbon film using an Edwards Auto 306 thermal evaporator. SEM operating conditions were an accelerating potential of 15 kV and a probe current of 500 pA.

1.7. Adsorption Process

Twenty-five milligrams of dried CSS was placed in 15 mL of NOR solution having a concentration of 10 mg/L at room temperature, before continuously stirring. One h was selected as the contact time to perform all of the adsorption experiments. The initial and final antibiotic concentration was monitored through UV−vis spectroscopy by applying the Lambert−Beer equation. Specifically, the absorbance maximum at 323 nm was considered with an ε value of 12740 L × mol × cm^{-1} (experimentally calculated). Therefore, the % of NOR adsorbed onto CSS was determined by adopting eq 1

$$\%\text{Ads} = \frac{C_0 - C_{60}}{C_0} \times 100 \quad (1)$$

in which C_0 and C_{60} indicate the NOR concentration at the beginning of the process and after 1 h in contact with CSS, respectively.

1.8. Determination of the CSS Point of Zero Charge (pH_{PZC})

A 30 mL portion of a 5.0 × 10^{-2} M NaCl solution was prepared by changing the pH values from 2 to 11 (pH_i, initial pH value) by adding an appropriate amount of HCl or NaOH. Then, the pH (pH_F, final pH value) of the solution was measured after contact with 25 mg of CSS for 48 h under continuous stirring. The pH_{PZC} value was obtained by reporting in the graph pH_i versus pH_i and pH_i versus

https://doi.org/10.1021/acsphyschemau.5c00013
ACS Phys. Chem Au 2025, 5, 375−386

pH_F; from the crossover of these curves, the pH_{PZC} value was experimentally inferred.

1.9. Photodegradation Experiments' Setup

For the NOR photodegradation, a UV fluorescent lamp (Spectroline, Model CNF 280C/FE, λ 254 nm, light flux 0.2 mW/cm^2) was used as a UV-light source. NOR photodegradation directly in water was assessed by placing 15 mL of the solution containing the pollutant, having an initial concentration of 10 mg/L, pH 7, under a UV lamp. A 100 mL beaker, kept under the lamp at 1 cm from the top, was used for this purpose, and the solution was continuously stirred. When used, TiO_2 and H_2O_2 were added directly into water. The UV−vis spectra were collected to monitor the NOR degradation induced by AOPs, and the % of degradation was inferred by determining the initial amount of the pollutant. About the photodegradation in the solid state, thus directly on CSS, the effects of UV light and UV light assisted by TiO_2 (for these experiments, 1 mg of TiO_2 was used) as a photocatalyst or H_2O_2 (0.005, 0.01, 0.1 M) as an oxidant agent were investigated. Specifically, after the adsorption of NOR on CSS (obtaining 50% of removed pollutant from water for each experiment), the adsorbent was collected, placed in 15 mL of fresh water, pH 7, and irradiated with UV light under stirring. Subsequently, the adsorbent material was recovered from the solution and used to desorb the non-photodestroyed pollutant in the presence of salt. Therefore, in this way, the amount of photodegraded NOR was indirectly inferred. In detail, the CSS was placed in 15 mL of a 0.1 M $MgCl_2$ solution and stirred for 30 min. Once again, the UV−vis spectra were acquired to monitor the NOR amount, and eq 2 was used to calculate the % of photodegraded NOR (% PD) in the solid state

$$\%PD = \frac{C_{Ads} - C_{Des}}{C_{Ads}} \times 100 \quad (2)$$

where C_{Ads} is the concentration of adsorbed NOR and C_{Des} is the concentration of desorbed NOR.

When TiO_2 and H_2O_2 were used to degrade NOR in the solid state, they were added directly into the water in which the adsorbent was placed. Finally, NOR photodegradation was also obtained simultaneously during its release in a 0.1 M $MgCl_2$ solution.1

2. RESULTS AND DISCUSSION

2.1. CSS Features

SEM, TGA, and ATR-FTIR analyses were carried out to investigate the CSS features to obtain information about its morphology, composition, and superficial functional groups before and after its use as an adsorbent substrate and recycling steps.

2.1.1. SEM Analysis. Macroscopically, raw CSS and CSS washed with water appeared as sawdust, having a yellowish color, with a smooth and compacted surface (see the camera picture reported in Figure 2A). In detail, SEM analyses revealed that raw CSS had a rough and heterogeneous surface made of flakes, characterized by cracks and covered by some impurities (Figure 2C,D). At the same time, according to the sampling regions (Figure 2C,D), they exhibited a wrinkled structure with an irregular surface with grooves, channeling, cracks, and nodules. After washing with water, the whole irregular morphology of CSS was retrieved, but the treatment compacted the structure due to a novel arrangement of the CSS network. Specifically, more characteristics can be appreciated in Figure 2E,F, confirming the findings. Indeed, the use of water for washing the biomass-based adsorbent should remove impurities, not affecting the entire characteristics of the material.

2.1.2. ATR-FTIR Spectroscopy Analyses. ATR-FTIR was performed to reveal the main functional groups on the CSS surface (Figure 3). According to other studies, the ATR-FTIR spectra showed the characteristic signals of cellulose, hemi-

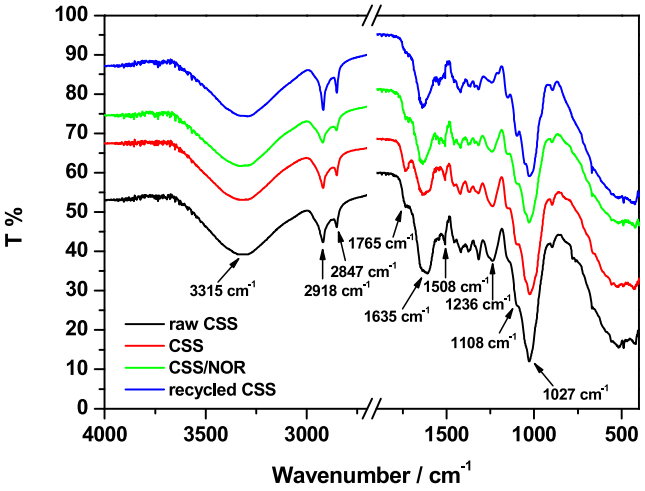

Figure 3. ATR-FTIR spectra (in the range between 4000 and 400 cm^{-1}) of raw CSS (black line), washed CSS (red line), CSS after NOR adsorption (green line), and CSS recycled for three adsorption and photodegradation cycles (blue line).

cellulose, and lignin.[40,41] Specifically, starting from raw CSS, the peak observed at 3315 cm^{-1} was associated with the O−H stretching of lignin phenols and the hydroxyl groups of cellulose and hemicellulose monosaccharides. The presence of two weak bands at 2918 and 2847 cm^{-1} was due to the symmetric and asymmetric stretching of the C−H bonds in the three polymers. The strong band at 1635 cm^{-1} and the weak peak at 1765 cm^{-1} could be ascribed to C═O vibrations of ketones, aldehydes, esters, and carboxylic acids.[42,43] Moreover, these signals could be correlated to the presence of other compounds, such as caffeine and chlorogenic acid.[40]

Specifically, starting from raw CSS, the peak observed at 3315 cm^{-1} was associated with the O−H stretching of lignin phenols and the hydroxyl groups of cellulose and hemicellulose monosaccharides. The presence of two weak bands at 2918 and 2847 cm^{-1} was due to the symmetric and asymmetric stretching of C−H bonds in the three polymers. The strong band at 1635 cm^{-1} and the weak peak at 1765 cm^{-1} could be ascribed to C═O vibrations of ketones, aldehydes, esters, and carboxylic acids.[42,43] Moreover, these signals could be correlated to the presence of other compounds, such as caffeine and chlorogenic acid.[40] The peaks at 1550−1200 cm^{-1} could include the C═C vibration in the aromatic ring of lignin[43] and the vibration modes of $-CH_3$, $-CH_2^-$, $-CH^-$ from cellulose, hemicellulose, and lignin, without excluding the involvement of C−O stretching of ether, phenol, and ester of lignin.[44] Lastly, the strong band at 1027 cm^{-1} and the shoulder at 1108 cm^{-1} could be due to the −C−O−C− vibration of glycosidic bonds between monosaccharides in cellulose and hemicellulose.[41] After the treatment of CSS with water, the ATR-FTIR spectrum appeared to be affected according to SEM analysis. In particular, the ratio intensity between the signals at 1745 cm^{-1} and 1635 cm^{-1} changed, showing an increase of the former, which appeared to be well-defined, and a reduction of the latter. At the same time, some variations were appreciated in the range 1425−1200 cm^{-1}. Therefore, by considering other similar studies reported in the literature,[45] the findings could indicate a rearrangement of the CSS

https://doi.org/10.1021/acsphyschemau.5c00013
ACS Phys. Chem Au 2025, 5, 375−386

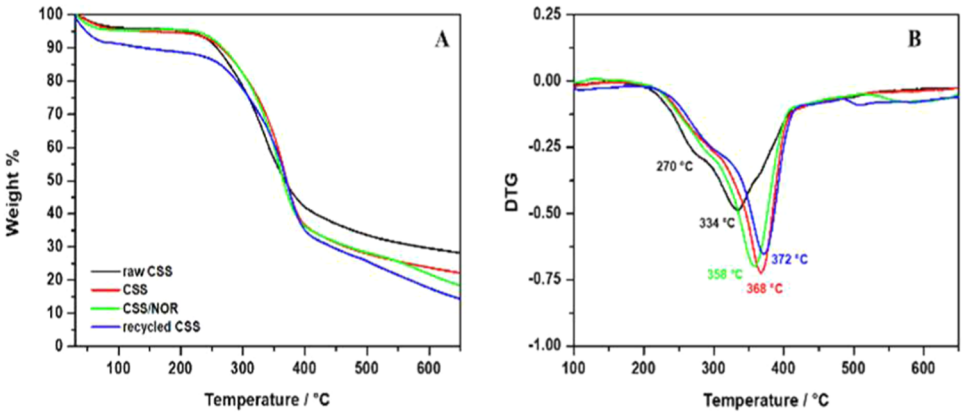

Figure 4. TGA (A) and related DTG curves (B) of raw CSS (black line); CSS washed with hot water (red line); CSS after NOR adsorption (green line); and CSS recycled for three adsorption and photodegradation cycles (blue line).

network, involving a new assembly of the biopolymer chains after water washing.[46]

2.1.3. Thermogravimetric Analyses. In excellent agreement with other works,[40,41,47,48] TGA curves of the investigated samples presented the typical signals of lignocellulosic materials (Figure 4A).

The raw CSS showed the first thermal event starting at 50−60 °C. It consisted of losing around 5% of the weight, and it could be correlated with the evaporation of surface-bound water.[40,47,48] Conversely, the most significant weight loss of 50% between 200 and 400 °C should involve the degradation of cellulose, hemicellulose, and lignin.[40,41] These weight losses characterized the corresponding Differential Thermogravimetric (DTG) curves (Figure 4B), causing the main broadband at 334 °C, with a less significant weight loss evidenced with a shoulder at 270 °C. Then, in the TGA curves at temperatures greater than 400 °C, 15% of the mass was lost, and the finding was attributed to lignin degradation.[42] At 650 °C, a residual mass of 30% was not degraded, and the signal could be assigned to the presence of nonburned inorganic compounds.[48]

After washing with water, the main CSS degradation stages started at higher temperatures, particularly at 230 °C, with a slight increase in weight loss to 60% (Figure 4A). At the same time, the maximum in the DTG curve of the observed broad signal shifted to 368 °C (Figure 4B). A similar behavior was observed in the literature, suggesting the reorganization of biopolymers in a new assembly, altered by the use of water, leading to an adsorbent more thermally stable if compared with raw CSS.[49−54] For instance, Benitez-Guerrero et al.[55] correlated the increase in thermal stability of another biomass, washed with hot water, to a better packing of the cellulose. Not surprisingly, the compacted morphology observed during the SEM investigation confirmed this result.

2.2. Adsorption of NOR onto CSS, and Desorption by Electrolyte Solutions

The UV−vis spectrum of NOR, whose molecular structure is reported in Figure 2B, is characterized by four main UV−vis absorbance maxima at 224, 273, 323, and 335 nm. These bands can be associated with $\pi \rightarrow \pi^*$ and $n \rightarrow \pi^*$ transitions arising from the pollutant functional groups. In particular, the absorbance at 224 nm could be attributed to the nicotinic moiety; instead, the maximum at 273 nm arises from the benzene ring and the carbonyl group. The maxima at 323 and 335 nm could be ascribed to the naphthalene group.[56] Therefore, these bands were considered diagnostic to follow the removal of NOR from water and its recovery from the adsorbent, along with its light-induced photodegradation. For instance, Figure 5A shows the time evolution of the UV−vis spectra of a NOR solution of 10 mg/L (15 mL) in contact with 25 mg of CSS, at pH 7. Eq 1 was thus used to calculate the % Ads at each reported contact time, and after 1 h, 50% of Norfloxacin was sequestered by CSS, evidencing the great performance of the used material.

Interestingly, after the first adsorption of NOR, the substrate morphology did not show important changes if compared with CSS washed with water before its use as an adsorbent. Indeed, images reported in Figure 2E,F were collected, denoting only the main effect of water on CSS morphology. According to this finding, the TGA showed slight differences in the thermal degradation curve of the adsorbent after the NOR removal compared with the curve related to CSS before its use (Figure 4A). Specifically, the DTG graph reveals that the main signal referring to cellulose, hemicellulose, and lignin occurred and shifted at lower temperature values (Figure 4B). Probably, NOR interacted with the lignocellulosic material, forming novel H-bonds and hydrophobic interactions, disturbing the previous ones, in favor of a less thermostable network. Accordingly, if as a whole the ATR-FTIR spectrum appeared similar to that before the NOR's adsorption (Figure 3), it showed important modifications: the ratio intensity between the signals 1745 cm^{-1} and 1635 cm^{-1} changes and the C═O contribution at 1740 cm^{-1} appears weaker, suggesting that the pollutant interacted with this functional group, probably involving lignin and hemicellulose. To get insight into the nature of interactions, the effect of pH on NOR's adsorption was studied (Figure 5B) at three pH values, i.e., pH 3, 7, and 12. The results obtained suggested that the adsorption was hindered at pH 3 and 12, whereas it improved at pH 7. To better understand these results, the point of zero charge of the material was at first purposely evaluated and occurred at around pH 6 (see the *inset* of Figure 5B), indicating that CSS, due to the presence of large number of carboxylic groups, was positively and negatively charged at pH <6 and pH >6, respectively. Particularly, the pH_{PZC} value was obtained by reporting in the graph pH_i versus pH_i and pH_i versus pH_F, as described in the Experimental Section; from the crossover of these curves, the pH_{PZC} value was inferred.

On the other hand, NOR has two pK_a values, $pK_{a1} \approx 6$ and $pK_{a2} \approx 8$, associated with the dissociation of the carboxylic

https://doi.org/10.1021/acsphyschemau.5c00013
ACS Phys. Chem Au 2025, 5, 375−386

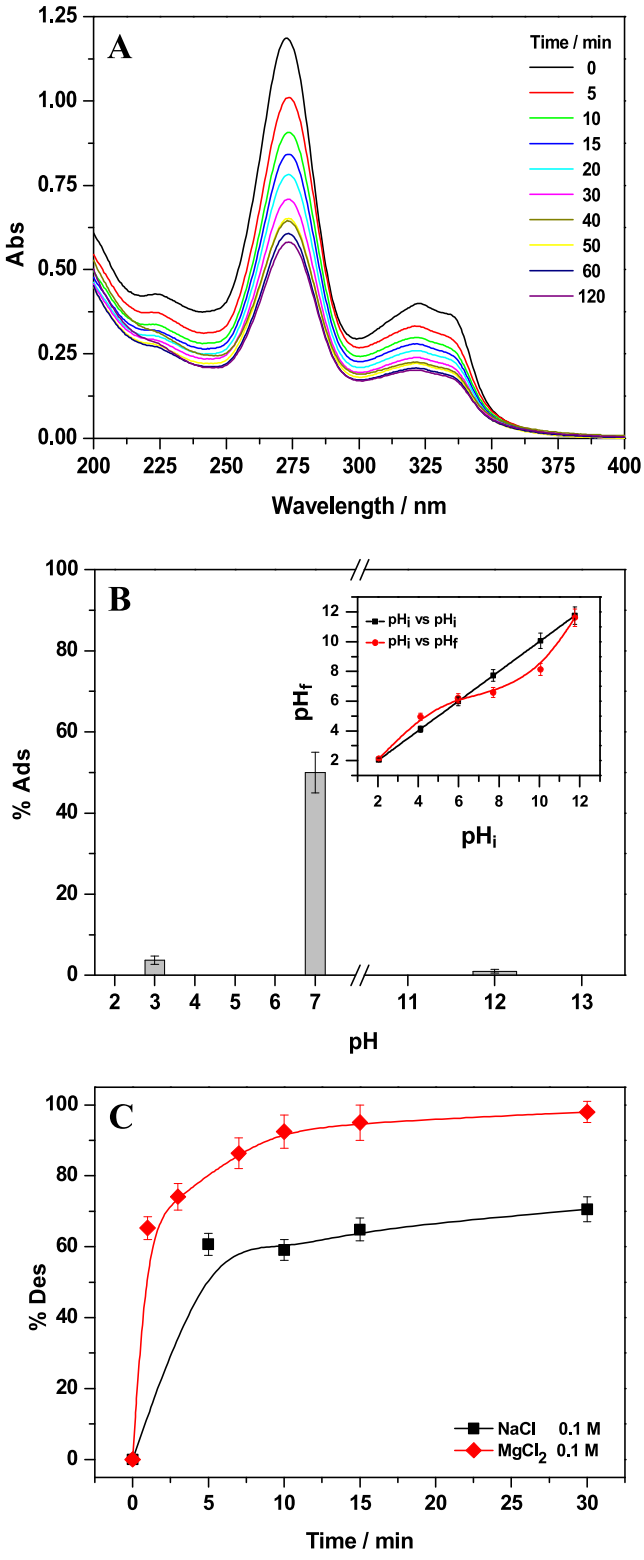

Figure 5. UV−vis spectra evolution of NOR during its adsorption onto CSS at reported contact time intervals (A); % of NOR removal at different pH values, and the adsorbent pH_{PZC} in the *inset* (B); % Des of adsorbed NOR on CSS placed into electrolyte solutions of NaCl and 0.1 M $MgCl_2$ (C). Adsorption conditions were 25 mg of CSS in contact with 15 mL of 10 mg/L NOR solution at room temperature.

groups and the nitrogen of the piperazinyl ring, respectively (see Figure 2B for the NOR molecular structure). Therefore, NOR can be considered a cation (NOR^+) at pH < pK_{a1}, zwitterion ($NOR^{\pm}$) in the range of pH between pK_{a1} < pH < pK_{a2}, or anion (NOR^-) at pH > pK_{a2}.[35,57] For this purpose, adsorption experiments were performed at three indicated pH values to study the contribution of NOR species, that changed according to the pH.[35,38]

In excellent agreement with the results reported in the literature, when biochar derived from spent coffee ground,[35] and coffee husk[38] were used, NOR occurred in water as zwitterion ($NOR^{\pm}$) at pH 7, and it was attracted by negatively charged CSS. For example, Paredes-Laverde et al.[38] attributed the finding to the presence of a large number of carboxylic groups on the adsorbent surface, as also observed herein during the ATR-FTIR analysis, which occurred to be deprotonated at this pH value. Therefore, the latter interacted with the protonated piperazinyl ring, favoring adsorption. Accordingly, by lowering and increasing the pH values, the repulsion between NOR and CSS, having the same charge, occurred, and the NOR removal from water was not observed (Figure 5B).

Once the CSS's adsorbent performance was assessed, a way to desorb the pollutant, quantifying its amount when photodegraded, was searched. Due to the presence of electrostatic forces between NOR and CSS, the use of salts appeared helpful, favoring an ionic exchange for releasing the pollutant. For this purpose, NaCl and 0.1 M $MgCl_2$ solutions were used, and the UV−vis spectroscopy helped to infer the concentration of desorbed NOR. Therefore, after the adsorption, the CSS was collected, washed with fresh deionized water to remove nonadsorbed NOR (monitored to eventually consider this amount), and then placed in the electrolyte solutions. As reported in Figure 5C, the use of $MgCl_2$ allowed the complete desorption of the adsorbed NOR in a very short time (in 15 min, the desorption can be considered to be quite complete), if compared with the use of the NaCl solution, in which only 70% was desorbed in 30 min of contact time. Probably, the small size of Mg^{2+}, as well as the associated ionic strength when present in water, and the well-known ability of NOR to coordinate Mg^{2+}, justified the results.[58] Therefore, the $MgCl_2$ solution of 0.1 M was used during the photodegradation experiment to desorb NOR and indirectly quantify the amount of destroyed pollutant, according to the working conditions adopted.

2.3. NOR Photodegradation: An Overview

The NOR photodegradation in water medium has already been ascertained in the literature, evidencing the clear oxidative mechanisms of reactions and the successful application of AOPs. In particular, Albini et al.[39] reported a work about the photophysics and photochemistry of fluoroquinolones. Degradation pathways were identified, rationalizing the results according to the molecular structure and adopted conditions of work. Evidence about the excited states involved in the direct photodegradation and the fragmentation modes was extensively described by the authors. On the other hand, in the environmental field, among the proposed approaches,[12,14,18−22] interesting results were obtained using UV light, UV/H_2O_2, UV/TiO_2, and UV/TiO_2/H_2O_2, which allow to have great degradation yield without sludge production.[18,19,21] In detail, if NOR is relatively stable under the use of only UV light and 3 h is necessary to remove the pollutant from water,[59] the addition of TiO_2 in the water enhanced the process.[21]

https://doi.org/10.1021/acsphyschemau.5c00013
ACS Phys. Chem Au 2025, 5, 375−386

Therefore, the contribution of the direct photolysis,[39] if present, under the adopted working conditions, was not the main mechanism, due to the reported slow NOR photodegradation. Conversely, the important role of the AOPs arose. Specifically, the use of the photocatalyst Degussa P25 has been reported to be more efficient if compared with other TiO_2-based powders. Interestingly, Jin et al.[60] showed that NOR could be potentially destroyed by following two degradation pathways, including the replacement of F atoms by hydroxyl radicals, piperazinyl ring cleavage, hydroxylation, and decarboxylation. Accordingly, during this work, a 10 mg/L NOR solution, at pH 7, when the molecule occurred mainly as a zwitterion,[39] was irradiated for 120 min with UV light and TiO_2 (Figure 6). The main absorption bands of NOR reduced

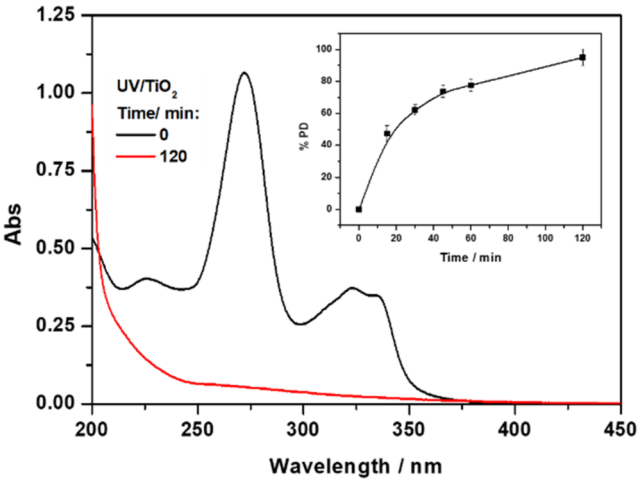

Figure 6. UV−vis spectra of a NOR solution (10 mg/L) before and after UV irradiation in the presence of TiO_2. *Inset:* % of photodegraded NOR at several irradiation times (i.e., 15, 30, 45, 60, 120 min).

their intensity due to complete antibiotic degradation. The *inset* in Figure 6 illustrates the % of photodegradation at several exposure times, showing an increase in degradation rate when extending the irradiation time. This finding was attributed to the overproduction of hydroxyl radicals that reacted with the antibiotic.[21,39] The addition of H_2O_2 improved the results: the degradation of NOR occurred in 60 min (data not shown), in excellent agreement with the literature.[18,19]

Based on these considerations, the NOR photodegradation on CSS was studied, also investigating the possibility of desorbing and then degrading the pollutant for adsorbent regeneration.

2.3.1. Solid-State Photodegradation of Adsorbed NOR on CSS. *2.3.1.1. Effect of UV Light and TiO_2.* As a first step, the photodegradation of NOR adsorbed onto CSS was performed under UV light, and the percentage of photodegraded NOR was calculated using eq 2, in which the difference between the adsorbed and released NOR amounts was considered.

After 1 h of exposure to UV light, 14% of adsorbed NOR was destroyed (Figure 7A). Considering the results obtained when the antibiotic was irradiated directly in the aqueous solution, the application of the UV light alone was unsatisfactory, confirming the low contribution of the NOR in direct photodegradation. Then, the action of UV light and TiO_2 was examined. Setting the exposure time to 1 h, an improvement in the % PD was found; indeed, the efficiency of photodegradation, compared with the result obtained with the simple UV-light irradiation, increased from 14 to 42% due to the large oxidant action caused by the generation of holes and electrons on TiO_2. The holes have a great oxidant potential, which could oxidize different chemicals; instead, the electrons could contribute to the generation of $^{\bullet}OH$ and $^{\bullet}O_2^-$ radicals that can react with NOR.[19,39] It is important to highlight that the adopted experimental conditions were the same as those adopted during the NOR degradation in water, but the observed % of PD values was lower, and the finding can be rationalized by considering that the pollutant degradation was performed at a solid state on CSS. The loaded adsorbent was placed in water in which TiO_2 was suspended; therefore, the production of radicals occurred mainly in the liquid phase at the interface of TiO_2/water and TiO_2/water/CSS. Moreover, the lignocellulosic CSS could behave as a scavenger of the oxidative agents, as demonstrated when the features of CSS were studied after the NOR removal, retarding the whole photodegradation in solid state, as herein observed.

Comparable behavior was already observed in the literature during the solid-state degradation of Ciprofloxacin, another antibiotic having a molecular structure similar to that of NOR, when adsorbed on Kiwi Peels.[45] Consequently, to improve the results obtained, the irradiation time was extended to 6 h. For the sake of comparison, the NOR photodegradation process was investigated at 0.5, 1, 2, 3, and 6 h. The results are reported in Figure 7A, which show a time-responsive behavior: the NOR photodegradation increased, reaching 60 and 100% after 3 and 6 h of irradiation time, respectively. To better evidence the obtained result, the UV−vis spectra of the released NOR after 6 h of irradiation, if in the presence of TiO_2, are reported in the *inset* of Figure 7A: the lack of signals ascribed to NOR after the desorption in $MgCl_2$ can be observed. Thus, according to the literature,[21] the use of UV light and TiO_2 was demonstrated as a powerful approach, but a prolonged time was necessary to obtain the complete NOR degradation.

2.3.1.2. Effect of UV/H_2O_2. For this purpose, three different concentrations of H_2O_2 were used for the NOR photodegradation, i.e., 0.005, 0.01, and 0.1 M, with the irradiation time set at 1 h. It is important to highlight that experiments showed that the molecules were stable in the absence of UV light. On the other hand, when UV light was used, the % PD was calculated and plotted in Figure 7B, showing that the photodegradation rate, if at minor extent, increased by raising the oxidant agent amount, as already observed in water solutions by de Souza Santos et al.[19] Then, the slight % PD enhancement would be correlated with the increase in $^{\bullet}OH$ production. Differently from the direct NOR photodegradation in water, in which the oxidant agent addition largely enhanced the degradation performance, favoring the quite complete NOR degradation,[18,19] in the solid state, the % PD was rather low. The finding confirmed the previous hypothesis discussed during the use of UV light and TiO_2. Specifically, the slight increase in % PD efficiency could be attributed to the fact that H_2O_2 was dissolved in the water surrounding the adsorbent.[44] Therefore, H_2O_2 in the solution absorbed UV light, and its photolysis occurred directly in water to produce hydroxyl radicals, as is well-known in the literature.[18,19] The latter not only easily reacted with each other but also can be quenched by CSS, not favoring the NOR degradation. Indeed, when the amount of H_2O_2 was low, no change with respect to the % PD

https://doi.org/10.1021/acsphyschemau.5c00013
ACS Phys. Chem Au 2025, 5, 375−386

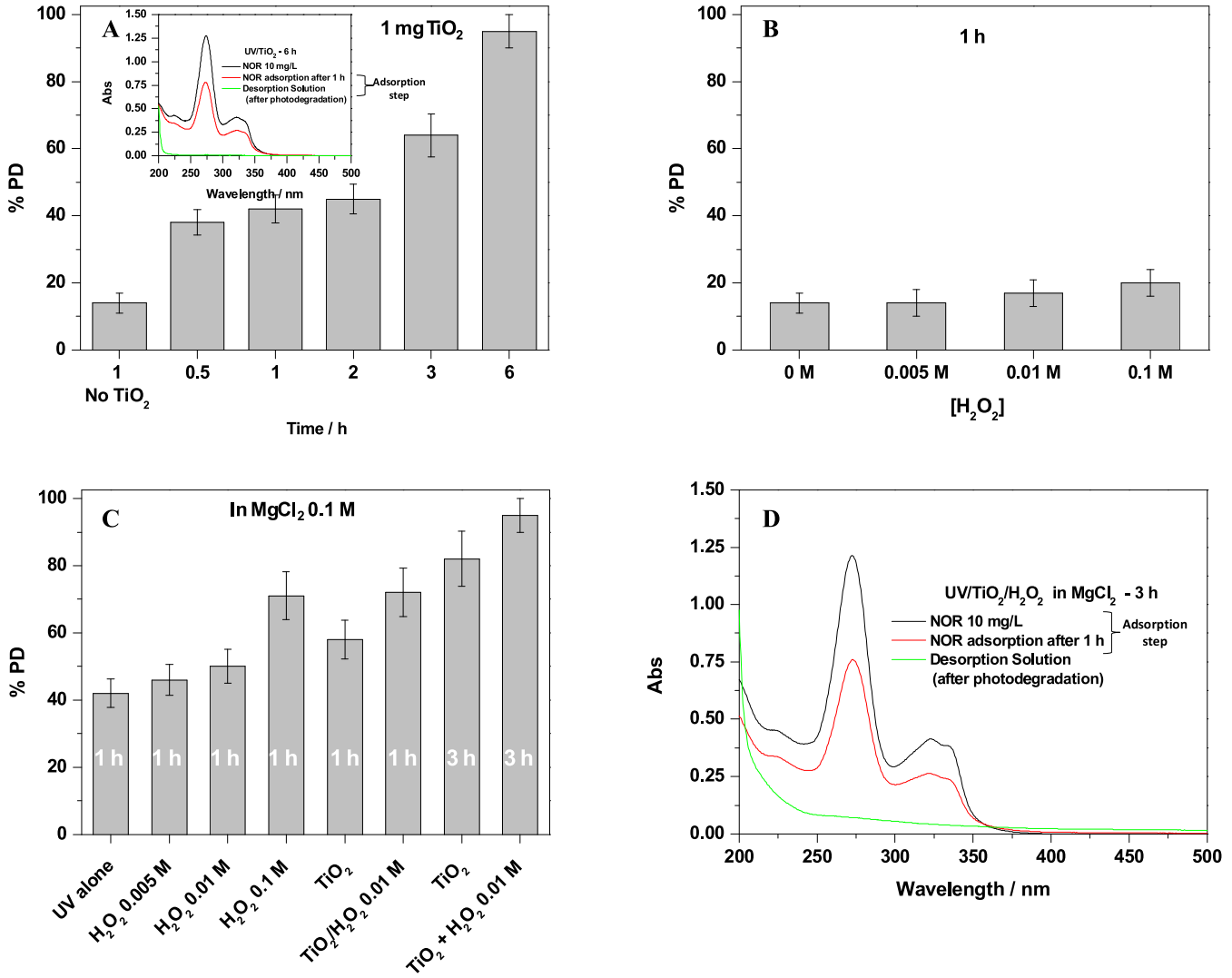

Figure 7. Percentage of photodegraded NOR after the adsorption on CSS in 15 mL of deionized water and 1 mg of TiO_2 at different irradiation times. *Inset*: spectra of NOR, related to photodegradation, with 6 h as the irradiation time (A); in solutions of H_2O_2 at different concentrations (i.e., 0, 0.005, 0.01, 0.1 M), fixing the irradiation time to 1 h (B); in 0.1 M $MgCl_2$ at different conditions (C). UV−vis spectra refer to experiments of NOR photodegradation performed during its release from CSS in the $MgCl_2$ solution when UV/TiO_2/H_2O_2 was applied for 3 h (D).

obtained with the lone use of UV light was observed; only the increase of H_2O_2 concentration favored the slight improvement.

Therefore, if the use of H_2O_2 in aqueous solutions can be considered beneficial, when the reactions occurred in a solid state, the presence of the oxidative agent was not suggested, and the use of UV light and TiO_2 occurred more powerfully, even if longer irradiation times were necessary. To overcome this negative aspect, an alternative approach is herein proposed, evaluating the possibility of desorbing NOR and, at the same time, favoring its photodegradation.

2.3.2. Simultaneous NOR Desorption from CSS in $MgCl_2$ and Photodegradation. Since NOR can be desorbed from CSS by using a $MgCl_2$ solution, the AOPs, previously adopted, were tested again during the NOR desorption. As reported in Figure 5B, NOR can be completely desorbed in a few minutes by using 0.1 M $MgCl_2$. Thus, the photodegradation in the solid state was performed under these conditions, with the aim of boosting the degradation of NOR. The results are reported in Figure 7C. Starting from the use of UV light alone and fixing the irradiation time at 1 h, the % PD increased from 14% (when destroyed at solid state) to 42% when released in a 0.1 M $MgCl_2$ solution (Figure 7C). This finding highlighted that the NOR release was advantageous: it improved the pollutant photodegradation rate, considering the involvement of the desorbed molecules in the solution, more exposed to the UV light than the adsorbed ones. Thus, to boost the process, 1 mg of TiO_2 was suspended in a solution containing the loaded adsorbent. In this condition, after 1 h of irradiation, the degradation percentage increased from 42% to around 60% (Figure 7C). On this basis, the irradiation time was extended to 3 h, observing that the % PD increased from 60 to 85%. The addition of H_2O_2, as expected when the pollutant was destroyed directly in water,[18] improved the result. Specifically, by adopting 0.01 M H_2O_2 in the presence of TiO_2, the complete degradation of adsorbed NOR was achieved by exposing CSS to UV light for 3 h (Figure 7D). Hence, differently from the results observed in the absence of the electrolyte, in this case, the release of NOR reduced the self-quenching of $^{\bullet}OH$, which, in turn, oxidized the pollutant molecules, boosting the process.

https://doi.org/10.1021/acsphyschemau.5c00013
ACS Phys. Chem Au 2025, 5, 375−386

2.4. CSS Recycling

To assess the possibility of reusing the adsorbent after its regeneration, consecutive cycles of NOR adsorption and degradation were performed. Specifically, for regenerating the adsorbent, the use of UV light and TiO_2 in the presence of 0.1 M $MgCl_2$ was selected, fixing the contact time at 3 h. Although the addition of H_2O_2 enhanced the process, as previously demonstrated, its use was avoided to extend the lifetime of the adsorbent that, as will be discussed later, was slightly affected by the oxidative conditions of the work. For each cycle, 25 mg of CSS was placed in a fresh NOR solution of 10 mg/L for 1 h as contact time, under stirring. Then, CSS was collected and washed with fresh deionized water to remove the nonadsorbed NOR, and it was placed in a fresh solution of 0.1 M $MgCl_2$, in which 1 mg of TiO_2 was added. Therefore, to explore the reusability of CSS, adsorption and photodegradation cycles were alternated with each other for 3 cycles. The % of adsorbed NOR (% Ads) and % of photodegraded NOR were calculated using eqs 1 and 2, respectively, and the results are reported in Figure 8. Clearly, the approach followed did not alter the performance of the adsorbent, since % of Ads and % PD remained the same during its reuse, opening a new horizon in CSS use and regeneration.

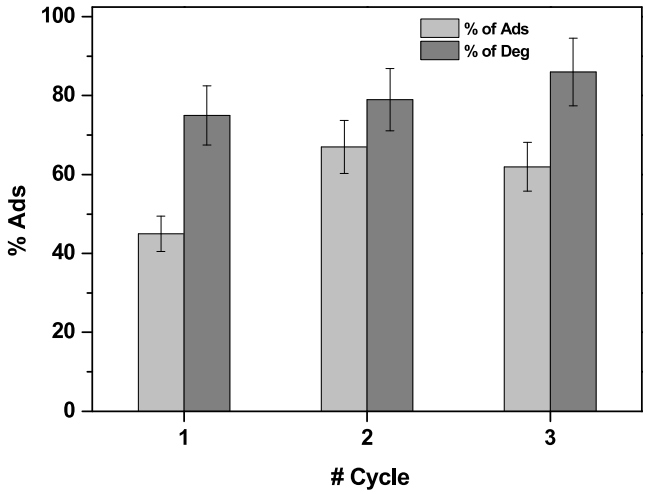

Figure 8. Percentage of adsorbed NOR onto CSS and % of degraded NOR after adsorption on CSS at different adsorption and photodegradation cycles. The adsorption was performed by placing 25 mg of CSS in 15 mL of a 10 mg/L NOR solution for 1 h; the photodegradation was carried out in 15 mL of a 0.1 M $MgCl_2$ solution and 1 mg of TiO_2, adopting 3 h as the irradiation time.

2.4.1. CSS Features after the Recycling Step. SEM, ATR-FTIR, and TGA were performed on the recycled adsorbent to characterize it. SEM images (Figure 2G,H) revealed that the CSS morphology was discovered after the recycling, and the finding can be attributed to the use of the adopted approaches that, as expected, can affect lignocellulosic materials.[61,62] Although the adsorbent was repeatedly washed with water, the presence of TiO_2 as microagglomerate particles can also be appreciated on the CSS surface. The ATR-FTIR analyses reported in Figure 3 show that the bands at 2918 and 2847 cm^{-1}, attributed to the C−H symmetric and asymmetric stretching in the lignocellulosic adsorbent, respectively, occurred to be well-defined and intense after the reuse of the adsorbent. At the same time, the weak peak at 1765 cm^{-1} ascribed to C═O vibrations of ketones, aldehydes, esters, and carboxylic acids was slightly evident. The peaks in the range of 1550−1200 cm^{-1}, which include the C═C vibration of the aromatic ring of lignin, the vibration modes of CH_3^-, $-CH_2^-$, and $-CH^-$ from cellulose, hemicellulose, and lignin, and the involvement of C−O stretching of ether, phenol, and ester of lignin, were affected. Particularly, the decrease in intensity of the peak at 1260 cm^{-1} could be correlated to the lignin oxidation, confirming the hypothesis about the role of CSS as an oxidant scavenger.[63] Accordingly, slight changes in the material's thermal decomposition profile were observed. Specifically, in the DTG analysis (Figure 4B), the main peaks' result shifted to a higher temperature, suggesting an alteration of hemicellulose and lignin functional groups.[64] Indeed, a slight contribution at 550 °C was detected and attributed to lignin by-products; probably, the used approach favored the cleavage of the aryl ether bonds in lignin,[63] leading to lower-weight lignin by-products, which usually display higher thermal instability.[65]

3. CONCLUSIONS

This work aims to valorize Coffee Silver Skin, a by-product of coffee torrefaction, as an adsorbent material for the removal of Norfloxacin from water. In particular, the recycling of the adsorbent with AOPs was successfully performed. The CSS was preliminarily characterized by using SEM, ATR-FTIR, and TGA, inferring information about its heterogeneous and rough surface and the lignocellulosic composition. For the CSS recycling, the application of different UV-light-based AOPs was investigated to photodegrade the adsorbed NOR; the addition of TiO_2 in the solution containing the adsorbent favored the process, whereas the use of H_2O_2 hindered the process. A comparison with the NOR behavior when irradiated directly in water was thus performed to gain information about the proposed degradation on the CSS surface in the solid state. With the aim of reducing the exposure times to UV light, the NOR photodegradation was exploited during its release from CSS, thanks to the addition of 0.1 M $MgCl_2$. This procedure demonstrated not only the possibility of adsorbing the pollutant but also proposed a simple way to desorb the adsorbed NOR from CSS through the use of an electrolyte. Therefore, after exposing loaded CSS to UV light for 3 h in the electrolyte solution and in the presence of TiO_2, 80% of adsorbed NOR was photodegraded. The process could be improved by adding H_2O_2 to the water solution at a concentration of 0.1 M, allowing complete photodegradation of the antibiotic. However, to avoid the use of strong oxidative conditions, the use of UV/TiO_2 and a $MgCl_2$ solution was chosen as an approach to recycling CSS for various adsorption/photodegradation cycles. Although SEM, ATR-FTIR, and TGA showed an alteration of adsorbent material after the recycling step due to the oxidative medium of the lignocellulosic material, the adsorption performance remained the same, allowing us to consider this system suitable for removing NOR from water. In summary, CSS could be used to adsorb NOR from water and induce photodegradation in the solid state, avoiding the direct degradation of pollutants in water with the release of undesired by-products; thus, better control of the photodegradation treatment should be obtained.

https://doi.org/10.1021/acsphyschemau.5c00013
ACS Phys. Chem Au 2025, 5, 375−386

AUTHOR INFORMATION

Corresponding Author

Jennifer Gubitosa − *Dipartimento di Chimica, Università degli Studi "Aldo Moro" di Bari, 70126 Bari, Italy; CNR NANOTEC − Istituto di Nanotecnologia − Sede Secondaria di Bari c/o Dipartimento di Chimica, Università degli Studi di Bari "Aldo Moro", 70126 Bari, Italy;* orcid.org/0000-0001-8332-5772; Phone: +390805443443; Email: jennifer.gubitosa@uniba.it

Authors

Domenico Cignolo − *Dipartimento di Chimica, Università degli Studi "Aldo Moro" di Bari, 70126 Bari, Italy*

Vito Rizzi − *Dipartimento di Chimica, Università degli Studi "Aldo Moro" di Bari, 70126 Bari, Italy; Consiglio Nazionale delle Ricerche CNR-IPCF, UOS Bari, 70126 Bari, Italy*

Maria Teresa Bozzelli − *Dipartimento di Chimica, Università degli Studi "Aldo Moro" di Bari, 70126 Bari, Italy*

Paola Fini − *Consiglio Nazionale delle Ricerche CNR-IPCF, UOS Bari, 70126 Bari, Italy*

Andrea Petrella − *Department of Civil, Environmental, Land, Construction and Chemistry, Polytechnic University of Bari, Bari 70125, Italy*

Pinalysa Cosma − *Dipartimento di Chimica, Università degli Studi "Aldo Moro" di Bari, 70126 Bari, Italy; Consiglio Nazionale delle Ricerche CNR-IPCF, UOS Bari, 70126 Bari, Italy;* orcid.org/0000-0003-3018-4069

Complete contact information is available at: https://pubs.acs.org/10.1021/acsphyschemau.5c00013

Author Contributions

The manuscript was written through the contributions of all authors. All authors have given approval to the final version of the manuscript. CRediT: **Domenico Cignolo** data curation, investigation, writing - original draft; **Vito Rizzi** conceptualization, funding acquisition, validation; **Maria Teresa Bozzelli** investigation; **Paola Fini** data curation; **Andrea Petrella** data curation; **Pinalysa Cosma** funding acquisition, visualization; **Jennifer Gubitosa** data curation, methodology, supervision, writing - review & editing.

Funding

This work was supported by the following projects: "PRIN2022 con il finanziamento del Ministero dell'Università e della Ricerca nell'ambito del Bando relativo allo scorrimento delle graduatorie finali del bando PRIN2022" titled "From wastes to gold nanoparticles: CHemistRY for Sustainable And Low environmental Impact bio-circular Strategies in cancer therapy (CHRY.S.A.L.I.S.)"; PRIN2022-PNNR, "Finanziato dall'Unione europea − Next Generation EU" titled "Bioderived and atomic scale engineered natural adsorbents: from water remediation to hydrogen evolution" (BECOMEH2); "MICS" (Made in Italy − Circular and Sustainable) Extended Partnership and received funding from the European Union Next-Generation EU (PIANO NAZIONALE DI RIPRESA E RESILIENZA (PNRR)—MISSIONE 4 COMPONENTE 2, INVESTIMENTO 1.3—D.D. 1551.11-10-2022, PE00000004); PRIN2022 "New crosslinked cyclodextrin-based MOFs for the removal of Emerging Contaminants".

Notes

The authors declare no competing financial interest.

ACKNOWLEDGMENTS

We kindly acknowledge Dr. Giuseppe Di Cuia for his support in providing Coffee silverskin by "Fattoria Gallorosso," Contrada Murge S. Andrea Snc -75024 Montescaglioso (MT). We would also like to thank Adriano Boghetich for performing the SEM analysis.

REFERENCES

(1) Lajunen, T. J. Antibiotic Use in Communities. *Antibiotics* **2024**, *13*, No. 438.

(2) Karampela, I.; Dalamaga, M. Could Respiratory Fluoroquinolones, Levofloxacin and Moxifloxacin, Prove to Be Beneficial as an Adjunct Treatment in COVID-19? *Arch. Med. Res.* **2020**, *51* (7), 741−742.

(3) Bhatt, S.; Chatterjee, S. Fluoroquinolone Antibiotics: Occurrence, Mode of Action, Resistance, Environmental Detection, and Remediation − A Comprehensive Review. *Environ. Pollut.* **2022**, *315*, No. 120440.

(4) Georgin, J.; Franco, D. S. P.; Meili, L.; Bonilla-Petriciolet, A.; Kurniawan, T. A.; Imanova, G.; Demir, E.; Ali, I. Environmental Remediation of the Norfloxacin in Water by Adsorption: Advances, Current Status and Prospects. *Adv. Colloid Interface Sci.* **2024**, *324*, No. 103096.

(5) Sauvé, S.; Desrosiers, M. A Review of What Is an Emerging Contaminant. *Chem. Cent. J.* **2014**, *8* (1), No. 15.

(6) de Souza, D. I.; Dottein, E. M.; Giacobbo, A.; Siqueira Rodrigues, M. A.; de Pinho, M. N.; Bernardes, A. M. Nanofiltration for the Removal of Norfloxacin from Pharmaceutical Effluent. *J. Environ. Chem. Eng.* **2018**, *6* (5), 6147−6153.

(7) Zhou, X.; Lu, L.; Li, X.; Meng, F.; Ding, Z.; Li, Z.; Chen, B.; Zhang, J. Mechanism and Effect of Magnetic Biochar on the Removal of Norfloxacin from Water by Ozone Peroxidation Adsorption-Coagulation Process. *J. Water Process Eng.* **2025**, *69*, No. 106655.

(8) Srinivasa Raghavan, D. S.; Qiu, G.; Ting, Y.-P. Fate and Removal of Selected Antibiotics in an Osmotic Membrane Bioreactor. *Chem. Eng. J.* **2018**, *334*, 198−205.

(9) Zhao, R.; Li, X.; Hu, M.; Li, S.; Zhai, Q.; Jiang, Y. Efficient Enzymatic Degradation Used as Pre-Stage Treatment for Norfloxacin Removal by Activated Sludge. *Bioprocess Biosyst. Eng.* **2017**, *40* (8), 1261−1270.

(10) Dorival-García, N.; Zafra-Gómez, A.; Navalón, A.; González, J.; Vílchez, J. L. Removal of Quinolone Antibiotics from Wastewaters by Sorption and Biological Degradation in Laboratory-Scale Membrane Bioreactors. *Sci. Total Environ.* **2013**, *442*, 317−328.

(11) Ohale, P. E.; Igwegbe, C. A.; Iwuozor, K. O.; Emenike, E. C.; Obi, C. C.; Białowiec, A. A Review of the Adsorption Method for Norfloxacin Reduction from Aqueous Media. *MethodsX* **2023**, *10*, No. 102180.

(12) Guo, H.; Ke, T.; Gao, N.; Liu, Y.; Cheng, X. Enhanced Degradation of Aqueous Norfloxacin and Enrofloxacin by UV-Activated Persulfate: Kinetics, Pathways and Deactivation. *Chem. Eng. J.* **2017**, *316*, 471−480.

(13) Chen, X.; Wang, J. Degradation of Norfloxacin in Aqueous Solution by Ionizing Irradiation: Kinetics, Pathway and Biological Toxicity. *Chem. Eng. J.* **2020**, *395*, No. 125095.

(14) Sayed, M.; Khan, J. A.; Shah, L. A.; Shah, N. S.; Khan, H. M.; Rehman, F.; Khan, A. R.; Khan, A. M. Degradation of Quinolone Antibiotic, Norfloxacin, in Aqueous Solution Using Gamma-Ray Irradiation. *Environ. Sci. Pollut. Res.* **2016**, *23* (13), 13155−13168.

(15) Teng, J.; Teng, R.; Jiang, J.; Hao, T.; Song, H.; Tan, W.; Shi, D.; Qin, H. Mechanism of Norfloxacin Adsorption on Fe-BTC Derived from Acid Mine Drainage Sludge: Adsorption Experiments and Density Functional Theory Analysis. *Langmuir* **2025**, *41* (5), 3643−3653.

(16) Zou, M.; Tian, W.; Chu, M.; Chen, Z. Effective Adsorption of Norfloxacin from Water on Magnetic Biochar Composite Derived from Cellulase Hydrolysis Apple Branch: Synthesis Optimization,

Performance Assessment and Mechanism Insight. *Process Saf. Environ. Prot.* **2024**, *185*, 435−444.
(17) Chen, W.; Li, X.; Zhao, P.; Zhu, X.; Deng, X. Preparation of Biomass Artificial Humic Acid/Hydrothermal Carbon Composite and Its High-Efficiency Adsorption of Norfloxacin. *J. Water Process Eng.* **2024**, *66*, No. 105924.
(18) Shankaraiah, G.; Poodari, S.; Bhagawan, D.; Himabindu, V.; Vidyavathi, S. Degradation of Antibiotic Norfloxacin in Aqueous Solution Using Advanced Oxidation Processes (AOPs)—A Comparative Study. *Desalin. Water Treat.* **2016**, *57* (57), 27804−27815.
(19) de Souza Santos, L. V.; Meireles, A. M.; Lange, L. C. Degradation of Antibiotics Norfloxacin by Fenton, UV and UV/H2O2. *J. Environ. Manage.* **2015**, *154*, 8−12.
(20) Wang, C.; Yu, G.; Chen, H.; Wang, J. Degradation of Norfloxacin by Hydroxylamine Enhanced Fenton System: Kinetics, Mechanism and Degradation Pathway. *Chemosphere* **2021**, *270*, No. 129408.
(21) Haque, M. M.; Muneer, M. Photodegradation of Norfloxacin in Aqueous Suspensions of Titanium Dioxide. *J. Hazard. Mater.* **2007**, *145* (1), 51−57.
(22) Wang, P.; Zhang, H.; Wu, Z.; Zhao, X.; Sun, Y.; Duan, N.; Liu, Z.; Liu, W. A Data-Based Review on Norfloxacin Degradation by Persulfate-Based Advanced Oxidation Processes: Systematic Evaluation and Mechanisms. *Chin. Chem. Lett.* **2023**, *34* (12), No. 108722.
(23) Abdel-Raouf, M. E.; Maysour, N. E.; Farag, R. K.; Abdul-Raheim, A.-R. M.Wastewater Treatment Methodologies, Review Article *Int. J. Environ. Agric. Sci.* 2019; Vol. 3018.
(24) Deng, Y.; Zhao, R. Advanced Oxidation Processes (AOPs) in Wastewater Treatment. *Curr. Pollut. Rep.* **2015**, *1* (3), 167−176.
(25) Babić, S.; Periša, M.; Škorić, I. Photolytic Degradation of Norfloxacin, Enrofloxacin and Ciprofloxacin in Various Aqueous Media. *Chemosphere* **2013**, *91* (11), 1635−1642.
(26) Skorupa, A.; Worwąg, M.; Kowalczyk, M. Coffee Industry and Ways of Using By-Products as Bioadsorbents for Removal of Pollutants. *Water.* **2023**, *15*, 112.
(27) Murthy, P. S.; Madhava Naidu, M. Sustainable Management of Coffee Industry By-Products and Value Addition—A Review. *Resour., Conserv. Recycl.* **2012**, *66*, 45−58.
(28) Sporchia, F.; Caro, D.; Bruno, M.; Patrizi, N.; Marchettini, N.; Pulselli, F. M. Estimating the Impact on Water Scarcity Due to Coffee Production, Trade, and Consumption Worldwide and a Focus on EU. *J. Environ. Manage.* **2023**, *327*, No. 116881.
(29) Liu, J.; Yang, H.; Gosling, S. N.; Kummu, M.; Flörke, M.; Pfister, S.; Hanasaki, N.; Wada, Y.; Zhang, X.; Zheng, C.; Alcamo, J.; Oki, T. Water Scarcity Assessments in the Past, Present, and Future. *Earth's Future* **2017**, *5* (6), 545−559.
(30) Schyns, J. F.; Hoekstra, A. Y.; Booij, M. J. Review and Classification of Indicators of Green Water Availability and Scarcity. *Hydrol. Earth Syst. Sci.* **2015**, *19* (11), 4581−4608.
(31) Blinová, L.; Sirotiak, M.; Bartošová, A.; Soldán, M. Review: Utilization of Waste From Coffee Production. *Res. Pap. - Fac. Mater. Sci. Technol., Slovak Univ. Technol.* **2017**, *25* (40), 91−101.
(32) Narita, Y.; Inouye, K. Review on Utilization and Composition of Coffee Silverskin. *Food Res. Int.* **2014**, *61*, 16−22.
(33) Tran, T. K. N.; Ngo, T. C. Q.; Nguyen, Q. V.; Do, T. S.; Hoang, N. B. Chemistry Potential and Application of Activated Carbon Manufactured from Coffee Grounds in the Treatment of Wastewater: A Review. *Mater. Today Proc.* **2022**, *60*, 1914−1919.
(34) Pagalan Jr, E., Jr; Sebron, M.; Gomez, S.; Salva, S. J.; Ampusta, R.; Macarayo, A. J.; Joyno, C.; Ido, A.; Arazo, R. Activated Carbon from Spent Coffee Grounds as an Adsorbent for Treatment of Water Contaminated by Aniline Yellow Dye. *Ind. Crops Prod.* **2020**, *145*, No. 111953.
(35) Nguyen, V.-T.; Vo, T.-D.-H.; Nguyen, T.-B.; Dat, N. D.; Huu, B. T.; Nguyen, X.-C.; Tran, T.; Le, T.-N.-C.; Duong, T.-G.-H.; Bui, M.-H.; Dong, C.-D.; Bui, X.-T. Adsorption of norfloxacin from aqueous solution on biochar derived from spent coffee ground: Master variables and response surface method optimized adsorption process. *Chemosphere* **2022**, *288*, No. 132577.
(36) Malara, A.; Paone, E.; Frontera, P.; Bonaccorsi, L.; Panzera, G.; Mauriello, F. Sustainable Exploitation of Coffee Silverskin in Water Remediation. *Sustainability* **2018**, *10*, 3547.
(37) Batista Meneses, D.; Montes de Oca-Vásquez, G.; Vega-Baudrit, J. R.; Rojas-Álvarez, M.; Corrales-Castillo, J.; Murillo-Araya, L. C. Pretreatment Methods of Lignocellulosic Wastes into Value-Added Products: Recent Advances and Possibilities. *Biomass Convers. Biorefinery* **2022**, *12* (2), 547−564.
(38) Paredes-Laverde, M.; Silva-Agredo, J.; Torres-Palma, R. A. Removal of norfloxacin in deionized, municipal water and urine using rice (*Oryza sativa*) and coffee (*Coffea arabica*) husk wastes as natural adsorbents. *J. Environ. Manage* **2018**, *213*, 98−108.
(39) Albini, A.; Monti, S. Photophysics and photochemistry of fluoroquinolones. *Chem. Soc. Rev.* **2003**, *32*, 238−250.
(40) Ballesteros, L. F.; Teixeira, J. A.; Mussatto, S. I. Chemical, Functional, and Structural Properties of Spent Coffee Grounds and Coffee Silverskin. *Food Bioprocess Technol.* **2014**, *7* (12), 3493−3503.
(41) Nolasco, A.; Squillante, J.; Velotto, S.; D'Auria, G.; Ferranti, P.; Mamone, G.; Errico, M. E.; Avolio, R.; Castaldo, R.; Cirillo, T.; Esposito, F. Valorization of Coffee Industry Wastes: Comprehensive Physicochemical Characterization of Coffee Silverskin and Multipurpose Recycling Applications. *J. Cleaner Prod.* **2022**, *370*, No. 133520.
(42) Waziri, S. A.; Dhada, I.; Das, R.A Comprehensive Database for Characterizing Potential of Common Biomass Feedstocks *Biomass Convers. Biorefinery* 2025 DOI: 10.1007/s13399-024-06459-4.
(43) Nabais, J. M. V.; Nunes, P.; Carrott, P. J. M.; Ribeiro Carrott, M. M. L.; García, A. M.; Díaz-Díez, M. A. Production of Activated Carbons from Coffee Endocarp by CO2 and Steam Activation. *Fuel Process. Technol.* **2008**, *89* (3), 262−268.
(44) Gubitosa, J.; Rizzi, V.; Cignolo, D.; Fini, P.; Fanelli, F.; Cosma, P. From Agricultural Wastes to a Resource: Kiwi Peels, as Long-Lasting, Recyclable Adsorbent, to Remove Emerging Pollutants from Water. The Case of Ciprofloxacin Removal. *Sustainable Chem. Pharm.* **2022**, *29*, No. 100749.
(45) Jiang, Z.; Yi, J.; Li, J.; He, T.; Hu, C. Promoting Effect of Sodium Chloride on the Solubilization and Depolymerization of Cellulose from Raw Biomass Materials in Water. *ChemSusChem* **2015**, *8* (11), 1901−1907.
(46) Iáñez-Rodríguez, I.; Martín-Lara, M. Á.; Pérez, A.; Blázquez, G.; Calero, M. Water Washing for Upgrading Fuel Properties of Greenhouse Crop Residue from Pepper. *Renewable Energy* **2020**, *145*, 2121−2129.
(47) Kumar, K. S.; Gairola, S.; Singh, I. Waste Coffee Silverskin as a Potential Filler in Sustainable Composites: Mechanical, Thermal, and Microstructural Analysis. *Ind. Crops Prod.* **2024**, *210*, No. 118088.
(48) Górska, A.; Brzezińska, R.; Wirkowska-Wojdyła, M.; Bryś, J.; Domian, E.; Ostrowska-Ligęza, E. Application of Thermal Methods to Analyze the Properties of Coffee Silverskin and Oil Extracted from the Studied Roasting By-Product. *Appl. Sci.* **2020**, *10*, No. 8790.
(49) Zhang, S.; Dong, Q.; Zhang, L.; Xiong, Y. Effects of Water Washing and Torrefaction on the Pyrolysis Behavior and Kinetics of Rice Husk through TGA and Py-GC/MS. *Bioresour. Technol.* **2016**, *199*, 352−361.
(50) Sebestyén, Z.; May, Z.; Réczey, K.; Jakab, E. The Effect of Alkaline Pretreatment on the Thermal Decomposition of Hemp. *J. Therm. Anal. Calorim.* **2011**, *105* (3), 1061−1069.
(51) Sebestyén, Z.; Jakab, E.; May, Z.; Sipos, B.; Réczey, K. Thermal Behavior of Native, Washed and Steam Exploded Lignocellulosic Biomass Samples. *J. Anal. Appl. Pyrolysis* **2013**, *101*, 61−71.
(52) Zhao, X.; Yang, F.; Tan, H.; Jiao, Y.; Zhou, M. Effect of the Water Washing Pretreatment on Biomass Pyrolysis in CO2 atm. *J. Energy Inst.* **2024**, *115*, No. 101697.
(53) Jiang, J.; Tie, Y.; Deng, L.; Che, D. Influence of Water-Washing Pretreatment on Ash Fusibility of Biomass. *Renew. Energy* **2022**, *200*, 125−135.
(54) Rodríguez-Machín, L.; Arteaga-Pérez, L. E.; Pérez-Bermúdez, R. A.; Casas-Ledón, Y.; Prins, W.; Ronsse, F. Effect of Citric Acid Leaching on the Demineralization and Thermal Degradation Behavior

of Sugarcane Trash and Bagasse. *Biomass Bioenergy* **2018**, *108*, 371−380.
(55) Benítez-Guerrero, M.; López-Beceiro, J.; Sánchez-Jiménez, P. E.; Pascual-Cosp, J. Comparison of Thermal Behavior of Natural and Hot-Washed Sisal Fibers Based on Their Main Components: Cellulose, Xylan and Lignin. TG-FTIR Analysis of Volatile Products. *Thermochim. Acta* **2014**, *581*, 70−86.
(56) Aura, R.; Silvia, I.; Eleonora, M.; Gabriel, H. Quinolone Antibacterials: Commentary and Considerations Regarding UV Spectra and Chemical Structure. *Acta Med. Marisiensis* **2015**, *61* (4), 328−336.
(57) Turel, I. The Interactions of Metal Ions with Quinolone Antibacterial Agents. *Coord. Chem. Rev.* **2002**, *232* (1), 27−47.
(58) Martínez, L.; Bilski, P.; Chignell, C. F. Effect of Magnesium and Calcium Complexation on the Photochemical Properties of Norfloxacin. *Photochem. Photobiol.* **1996**, *64* (6), 911−917.
(59) Liu, W.; He, T.; Wang, Y.; Ning, G.; Xu, Z.; Chen, X.; Hu, X.; Wu, Y.; Zhao, Y. Synergistic Adsorption-Photocatalytic Degradation Effect and Norfloxacin Mechanism of ZnO/ZnS@BC under UV-Light Irradiation. *Sci. Rep.* **2020**, *10* (1), No. 11903.
(60) Jin, X.; Zhou, X.; Sun, P.; Lin, S.; Cao, W.; Li, Z.; Liu, W. Photocatalytic Degradation of Norfloxacin Using N-Doped TiO2: Optimization, Mechanism, Identification of Intermediates and Toxicity Evaluation. *Chemosphere* **2019**, *237*, No. 124433.
(61) Llatance-Guevara, L.; Flores, N. E.; Barrionuevo, G. O.; Mullo Casillas, J. L. Waste Biomass Selective and Sustainable Photooxidation to High-Added-Value Products: A Review. *Catalysts* **2022**, *12*, No. 1091.
(62) Shiamala, L.; Vignesh, K.; Jaffar Ali, B. M. Sunlight Active TiO2-Bi2WO6 Photocatalyst Pretreatment of Biomass for Simultaneous Hydrolysis and Saccharification in Bioethanol Production. *Fuel* **2023**, *333*, No. 126332.
(63) Nada, A. M. A.; Abou Yousef, H.; El-Gohary, S. Thermal Degradation of Hydrolyzed and Oxidized Lignins. *J. Therm. Anal. Calorim.* **2002**, *68* (1), 265−273.
(64) Davaritouchaee, M.; Hiscox, W. C.; Martinez-Fernandez, J.; Fu, X.; Mancini, R. J.; Chen, S. Effect of Reactive Oxygen Species on Biomass Structure in Different Oxidative Processes. *Ind. Crops Prod.* **2019**, *137*, 484−494.
(65) De Sá, I. C.; Oliveira Silva, P. M.; Nossol, E.; Borges, P. H. S.; Lepri, F. G.; Semaan, F. S.; Dornellas, R. M.; Pacheco, W. F. Modified Dry Bean Pod Waste (Phaseolus Vulgaris) as a Biosorbent for Fluorescein Removal from Aqueous Media: Batch and Fixed Bed Studies. *J. Hazard. Mater.* **2022**, *424*, No. 127723.

https://doi.org/10.1021/acsphyschemau.5c00013
ACS Phys. Chem Au 2025, 5, 375−386